ACS APPLIED MATERIALS & INTERFACES

Research Article

www.acsami.org

Spectroscopic Characterization of Structural Changes in Membrane Scaffold Proteins Entrapped within Mesoporous Silica Gel Monoliths

Wade F. Zeno,[†] Silvia Hilt,[‡] Subhash H. Risbud,[†] John C. Voss,[‡] and Marjorie L. Longo*[,†]

[†]Department of Chemical Engineering and Materials Science and [‡]Department of Biochemistry and Molecular Medicine, University of California at Davis, Davis, California 95616, United States

Supporting Information

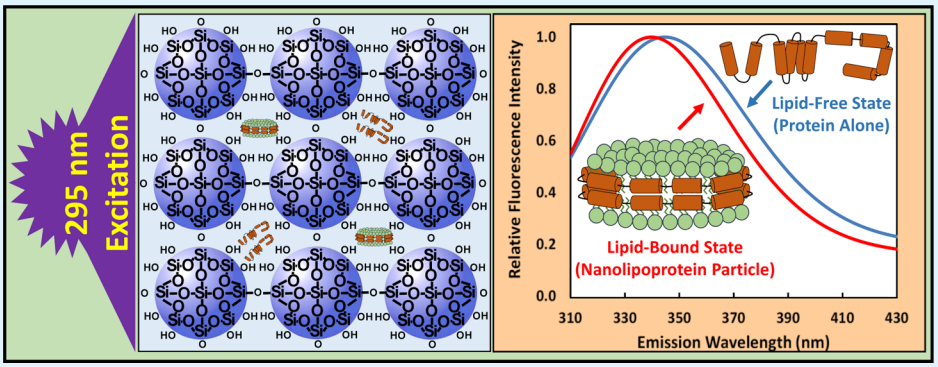

ABSTRACT: The changes in the orientation and conformation of three different membrane scaffold proteins (MSPs) upon entrapment in sol−gel-derived mesoporous silica monoliths were investigated. MSPs were examined in either a lipid-free or a lipid-bound conformation, where the proteins were associated with lipids to form nanolipoprotein particles (NLPs). NLPs are water-soluble, disk-shaped patches of a lipid bilayer that have amphiphilic MSPs shielding the hydrophobic lipid tails. The NLPs in this work had an average thickness of 5 nm and diameters of 9.2, 9.7, and 14.8 nm. We have previously demonstrated that NLPs are more suitable lipid-based structures for silica gel entrapment than liposomes because of their size compatibility with the mesoporous network (2−50 nm) and minimally altered structure after encapsulation. Here we further elaborate on that work by using a variety of spectroscopic techniques to elucidate whether or not different MSPs maintain their protein−lipid interactions after encapsulation. Fluorescence spectroscopy and quenching of the tryptophan residues with acrylamide, 5-DOXYL-stearic acid, and 16-DOXYL-stearic acid were used to determine the MSP orientation. We also utilized fluorescence anisotropy of tryptophans to measure the relative size of the NLPs and MSP aggregates after entrapment. Finally, circular dichroism spectroscopy was used to examine the secondary structure of the MSPs. Our results showed that, after entrapment, all of the lipid-bound MSPs maintained orientations that were minimally changed and indicative of association with lipids in NLPs. The tryptophan residues appeared to remain buried within the hydrophobic core of the lipid tails in the NLPs and appropriately spaced from the bilayer center. Also, after entrapment, lipid-bound MSPs maintained a high degree of α-helical content, a secondary structure associated with protein−lipid interactions. These findings demonstrate that NLPs are capable of serving as viable hosts for functional integral membrane proteins in the synthesis of sol−gel-derived bioinorganic hybrid nanomaterials.

KEYWORDS: *membrane scaffold protein, nanolipoprotein particle, mesoporous silica, tryptophan fluorescence, biohybrid material, protein−lipid interactions*

INTRODUCTION

The interface between biological species and inorganic materials serves as a platform for the development of many unique and interesting biomaterials. Encapsulation of functional proteins within mesoporous silica has been of particular interest to a wide variety of research areas over the last several decades because of its extensive applications,[1,2] as well as the ability of silica to protect the entrapped protein from denaturation and proteolytic hydrolysis.[3,4] More recently, there has been increasing interest in the entrapment of integral membrane proteins (IMPs) to synthesize biomaterials for applications such as biosensing, high-throughput drug screening, affinity chromatography, and bioreaction engineering.[5−7] This is due to the various functionalities of IMPs, which include enzymatic, transport, and receptor−ligand-binding activity.[8] IMPs, however, require a biological membrane (i.e., an amphipathic lipid bilayer) into which it can insert itself to maintain an active tertiary conformation.[8,9] It is well-known that the lack of a proper biological membrane or disruption of a lipid membrane bearing an IMP can result in inactivation of the IMP.[10−13]

Received: January 29, 2015
Accepted: April 7, 2015
Published: April 7, 2015

DOI: 10.1021/acsami.5b00898
ACS Appl. Mater. Interfaces 2015, 7, 8640−8649

Therefore, it is crucial to develop a biomembrane/sol−gel architecture such that the biological membrane host structure is minimally altered upon encapsulation.

To ensure viable incorporation of biological membranes, a sol−gel route must be biologically friendly. The desire for protein entrapment has served as an impetus for the development of biocompatible sol−gel methods. Research groups headed by Bright, Friedman, Kostic, and Brennan began examining the properties of several water-soluble proteins entrapped in silica gel monoliths during the 1990s.[14−17] This eventually led to techniques that included the use of additives, such as glycerol and sugar, to alter hydration of the protein.[18,19] However, this approach did not address the presence of elevated alcohol concentrations, which is problematic in biological systems. Typical sol−gel synthesis utilizes alkoxysilane precursors, such as tetramethylorthosilicate (TMOS) or tetraethylorthosilicate (TEOS). Upon hydrolysis of these precursors, methanol and ethanol are released from TMOS and TEOS, respectively.[20] Sufficiently high concentrations of alcohol are capable of denaturing proteins or causing lipid bilayers to interdigitate (i.e., become thinner).[21,22] The latter would directly affect the conformation of any IMPs being supported by the lipid bilayer. Brennan's group developed biocompatible sol−gel alkoxysilane precursors bearing sugar moieties and/or glycerol in place of alcohol groups.[23,24] This approach led to the direct reduction of alcohol liberated during hydrolysis reactions, as well as the prevention of the additives being leached from the gel. They would later apply this sol−gel architecture to examine the entrapment of liposomes as biological membrane hosts for IMPs and found that the liposomes ruptured after several days, as opposed to immediately when using the precursor TEOS.[25] The significantly different scale of liposomes (100 nm) in comparison to the porous structure (2−50 nm) of silica gels, in addition to the rather fragile capsulelike structure of liposomes, may have played an important role in the eventual disruption of entrapped liposomes.

We propose the use of nanolipoprotein particles (NLPs) as biological membrane hosts inside mesoporous silica. NLPs are disk-shaped patches of a lipid bilayer that have amphiphilic membrane scaffold proteins (MSPs) in contact with and shielding the hydrophobic lipid tails around the outer periphery of the particle, thus making the entire particle water-soluble. NLPs have an average thickness of 5 nm and have a tunable diameter that ranges from 10 to 25 nm based on the types of MSPs used.[26] The aqueous processing conditions of the sol−gel method make it amenable to the incorporation of water-soluble NLPs. Also, the pore size distribution of the silica gel, 5−50 nm, provides a compatible size match for NLPs. In 2014, we first reported the stability of NLPs entrapped within mesoporous silica, where it was demonstrated that NLPs served as more viable structures than liposomes upon entrapment in silica gel.[27] To date, that was the first and only publication describing the entrapment of NLPs in mesoporous silica gel monoliths. We performed detailed analysis of the lipid phase behavior of the NLP within the particles to find that it was minimally modulated upon entrapment in comparison to the phase behavior for lipids in liposomes and that liposomes were undergoing significant changes in size in comparison to NLPs. This behavior was observable for a time period in excess of 1 month. The conformation of the particular MSP used in that work, referred to as MSP-3 in this work, was also evaluated. We found that the MSP maintained a conformation where it perhaps continued to interact with the lipids after silica gel encapsulation (i.e., a lipid-bound conformation) for at least 1 week. The analysis performed for the MSP, however, only provided insight for the structure of the protein rather than insight into the orientation of the MSP and elucidation as to whether or not the protein−lipid interactions truly remained intact.

In this work, we investigate the stability of the protein−lipid interactions in NLPs upon entrapment in mesoporous silica to determine whether or not a variety of different MSPs maintain a lipid-bound conformation. Encapsulation was performed using a simple sol−gel processing method for TMOS that utilizes rotary evaporation to remove the majority of methanol, a method first presented by Ferrer et al.[28] and previously used for the entrapment of liposomal species.[29] We examined NLPs formed with three different types of Apolipoprotein A-I derived MSPs, each having different chain lengths. These MSPs were initially synthesized and made commercially available by the research group of Stephen G. Sligar.[30,31] The orientations of the MSPs were determined via fluorescence spectroscopy and quenching of tryptophan residues with acrylamide and two different nitroxide-spin-labeled stearic acids. Fluorescence anisotropy of the tryptophan residues was also used for determining the relative size of lipid-free and -bound MSPs inside the silica gel. Last, circular dichroism (CD) spectroscopy was used with two of the three MSPs to determine their secondary structure in lipid-free and -bound states. We found that the MSPs maintained protein−lipid interactions within the NLPs upon encapsulation in a manner such that the interactions were minimally altered from that in solution. In combination with our previous work, these results strongly indicate that the NLPs maintain their structure upon entrapment in silica gel.

MATERIALS AND METHODS

Materials. Lyophilized MSP1D1 (MSP-1) and MSP1D1ΔH5 (MSP-2) were purchased from Cube Biotech, Inc., while lyophilized MSP1E3D1 (MSP-3) was purchased from Sigma-Aldrich, Inc. MSP-1, MSP-2, and MSP-3 had chain lengths of 217 amino acids (25.3 kDa), 184 amino acids (21.5 kDa), and 277 amino acids (32.6 kDa), respectively. All MSPs were purchased with histidine tags attached to their N-termini. Tetramethylorthosilicate (TMOS; ≤99%), acrylamide (≥99%), sodium chloride (≥99%), sodium cholate (≥99%), imidazole (≥99%), *N*-acetyl-L-tryptophanamide, 5-DOXYL-stearic acid free radical (5-DOXYL), and 16-DOXYL-stearic acid free radical (16-DOXYL) were also purchased from Sigma-Aldrich, Inc. 1,2-Dimyristoyl-*sn*-glycero-3-phosphocholine (DMPC) was purchased in chloroform from Avanti Polar Lipids, Inc. Tris(hydroxymethyl)-aminomethane (Tris, MB grade) was purchased from USB Corp., while hydrochloric acid (12.1 M), sodium phosphate dibasic heptahydrate, and sodium fluoride were purchased from Fischer Scientific, Inc. Ni-NTA agarose used for NLP purification was purchased from 5 PRIME, Inc. All of the water used for these experiments was purified in a Barnstead Nanopure System (Barnstead Thermolyne, Dubuque, IA) and had a resistivity of 17.9 MΩ·cm or greater.

Synthesis of NLPs. NLPs bearing MSP-1, MSP-2, and MSP-3 as scaffold proteins were used for tryptophan fluorescence quenching and anisotropy experiments, as well as far-UV CD experiments. They were prepared as previously described[27] with modifications. Briefly, for a single preparation, 5 mg of DMPC stock was dried in a glass conical vial under mild vacuum for at least 4 h, then rehydrated in a buffer consisting of 40 mM sodium cholate, 20 mM Tris, and 100 mM NaCl (pH 7.4), and incubated at 37 °C for 30 min. MSP-1, -2, or -3 was then added to the mixture such that the mass ratio of lipid−protein was 5:2 for MSP-1 and MSP-2 and 5:1 for MSP-3. Next, the

DOI: 10.1021/acsami.5b00898
ACS Appl. Mater. Interfaces 2015, 7, 8640−8649

solubilized lipid−protein mixture was incubated at 4 °C for 20 min and then 37 °C for 20 min. This was repeated two additional times. Afterward, the mixture was transferred to a 10000 MWCO dialysis cartridge (Thermo Scientific, Rockford, IL), dialyzed against 20 mM Tris and 100 mM NaCl buffer (pH 7.4) at 4 °C for 48 h at 200 times the sample volume, and underwent three buffer exchanges during this time period. From that point on, the rest of the procedure was performed identically with that of the aforementioned protocol, where the resulting NLP mixture was purified using Ni-NTA agarose, eluted with an imidazole-based buffer, and dialyzed again for 24 h to remove imidazole, resulting in purified NLPs in 20 mM Tris and 100 mM NaCl buffer (pH 7.4).

Entrapment of NLPs in Silica Gel. NLP entrapment was performed as previously described[27] with slight modification. In a typical preparation, 7.6 mL of TMOS was combined with 5.6 mL of 0.002 M HCl (in water) in a beaker submerged in an ice bath and then subjected to probe tip sonication for 15 min. Afterward, rotary evaporation (340 mbar reduced pressure, 50 °C) was used for 20 min to remove methanol formed during the hydrolysis reactions. The mixture was then passed through a 0.45 μm filter, resulting in roughly 4 mL of translucent silica sol. The sol was then combined with 20 mM Tris, 100 mM NaCl buffer (pH 7.4), and an NLP sample of choice (1 part sol, 1 part buffer, and 1 part sample; 3 equal volume portions) and allowed to gel in a methacrylate cuvette. Gelation typically occurred within 5−10 min. Gel volumes were approximately 2.5 mL. For samples used in quenching experiments, quenchers were added to the NLP sample before being combined with the sol. Lipid-free MSPs were encapsulated in an identical manner. All gelled samples contained approximately 5% (v/v) methanol. The silica gel was confirmed to be mesoporous, containing pore sizes in the range of 2−50 nm via N_2 adsorption (see the Supporting Information, SI).

Tryptophan Accessibility to Solvent Determination via Acrylamide Quenching. The relative accessibility of a tryptophan residue to solvent can be determined by using the Stern−Volmer relationship[32,33] (eq 1), where F_0, F, K_{SV}, and [Q] are the fluorescence intensity in the absence of quencher, fluorescence intensity in the presence of quencher, Stern−Volmer constant, and quencher concentration, respectively.

$$\frac{F_0}{F} = K_{SV}[Q] + 1 \tag{1}$$

The Stern−Volmer relationship shows that the inverse of the relative fluorescence intensity is linearly proportional to the concentration of quencher used. Therefore, higher values of K_{SV} indicate that a tryptophan residue is more exposed to water (i.e., more efficiently quenched), while a lower K_{SV} value indicates that a tryptophan residue is less exposed to water (i.e., less efficiently quenched). The quencher used in these experiments was acrylamide, which is water-soluble.

For solution quenching, samples from stock solutions of lipid-free and -bound MSP-1, -2, or -3 were diluted to a 4 μM final MSP concentration (2.5 mL total volume) in a methacrylate cuvette and titrated with a stock solution of 4 M acrylamide in 25 μL increments until a final concentration of approximately 0.16 M acrylamide was reached in the sample. For gel quenching, five samples for each type of lipid-free and -bound MSP (30 different samples in total) were created with varying acrylamide concentrations (0−0.16 M acrylamide) and an MSP concentration of 4 μM. Gel emission spectra were corrected by performing control experiments with *N*-acetyl-L-tryptophanamide (see the SI).

For all samples, tryptophan was excited at 295 nm and emission spectra were recorded from 300 to 450 nm. Each plot was regressed to remove noise and determine the emission spectrum's maximum intensity and critical wavelength (see the SI). The maximum intensity from each emission scan with acrylamide present was normalized by the maximum intensity of the corresponding emission scan in which acrylamide was not present and used to fit eq 1. All measurements were carried out on a PerkinElmer LS 55 fluorescence spectrometer equipped with a PTP-1 fluorescence Peltier system (PerkinElmer, Inc., Waltham, MA). Each measurement was performed in triplicate at 22 ± 1 °C. A scan speed of 180 nm/min was used, and 5.0 nm slit widths were used for both the excitation and emission monochromators.

Tryptophan Position Determination via Parallax Analysis. The parallax method was used to estimate the average position of tryptophan residues in the three MSPs when bound to lipids in NLPs. Because of the height difference between the nitroxide spin label in the 5-carbon and 16-carbon positions, 5-DOXYL and 16-DOXYL quench tryptophan in the MSP belt with different efficiencies.[34,35] The height of a tryptophan from the center of a bilayer is given by eq 2.[36,37]

$$Z_{eff} = L_{cd} - \frac{\ln\left[\frac{(F_s/F_o)^2}{F_d/F_o}\right]/\pi C - 2L_{ds}^{\ 2} + 4L_{cd}^{\ 2}}{4(L_{ds} + L_{cd})} \tag{2}$$

Z_{eff}, L_{cd}, and L_{ds} are the effective tryptophan height, length between the bilayer center and deep quencher, and length between the deep and shallow quenchers, respectively. In this work, 5-DOXYL is the shallow quencher, while 16-DOXYL is the deep quencher. Values for L_{cd} and L_{ds} were estimated for our system to be 0.82 and 11.33 Å (see the SI). F_s/F_o and F_d/F_o represent the relative tryptophan emission intensities in samples containing 5-DOXYL and 16-DOXYL, respectively. C is the concentration of DOXYL per area of lipid bilayer. This was estimated using the measured concentrations of the scaffold proteins and the solution size of the NLPs (see the SI). Equation 2 accounts for the quenching of tryptophan from DOXYL present in both lipid leaflets (i.e., trans-bilayer quenching).

For solution quenching, a 2.5 mL NLP sample in a methacrylate cuvette (4 μM MSP) was titrated with a 10 mM stock solution of either 5-DOXYL or 16-DOXYL in ethanol. Titrations were performed in 3 μL increments until the final DOXYL concentration was 15 μM in the sample. For gel, multiple samples were created for each type of MSP (three each for MSP-1 and -2 and two for MSP-3). Each sample contained a different concentration of either 5-DOXYL or 16-DOXYL (0−15 μM) and 4 μM MSP.

For all samples, tryptophan was excited at 295 nm and emission spectra were recorded from 300 to 450 nm. Each plot was regressed to remove noise and determine the emission spectrum's maximum intensity and emission wavelength (see the SI). The maximum intensity from each emission scan with DOXYL present was normalized by the maximum intensity of the corresponding emission scan in which DOXYL was not present and was used to fit eq 2. All measurements were carried out on a PerkinElmer LS 55 fluorescence spectrometer equipped with a PTP-1 fluorescence Peltier system (PerkinElmer, Inc., Waltham, MA). Each measurement was performed in triplicate at 22 ± 1 °C. A scan speed of 180 nm/min was used, and 5.0 nm slit widths were used for both the excitation and emission monochromators. No quenching was observed for lipid-free MSPs over the DOXYL concentration ranges used because there were no lipid bilayers present into which DOXYL molecules could partition.

Fluorescence Anisotropy of Tryptophan in MSPs. Anisotropy values (r) are a measure of the relative rotational speed of a fluorescent molecule.[38] It is calculated as the difference in the fluorescence intensities of emitted parallel and perpendicular polarized light normalized by the entire intensity of light emitted, as shown in eq 3.

$$r = \frac{F_{\parallel} - F_{\perp}}{F_{\parallel} + 2F_{\perp}} \tag{3}$$

Solution and gel samples containing 4 μM MSP in methacrylate cuvettes were measured for their anisotropy values using a FluoroLog-3 FL3-22 spectrophotometer (Horiba, Ltd., Kyoto, Japan). An excitation wavelength of 295 nm was used for all samples, while the emission wavelength depended on the sample, varying from 340 to 349 nm. An excitation slit width of 5.0 nm and an emission slit width of 2.5 nm were used. All anisotropy values were measured at 22 ± 1 °C and were the average of 10 anisotropy measurements.

CD of MSPs. CD spectroscopy of MSPs was performed as previously described.[27] Briefly, lipid-free and -bound MSPs in 20 mM Tris and 100 mM NaCl buffer (pH 7.4) were exchanged into 25 mM phosphate and 100 mM NaF buffer (pH 7.4) via dialysis. CD spectra were obtained using a Jasco J-715 spectropolarimeter (JASCO, Easton,

DOI: 10.1021/acsami.5b00898
ACS Appl. Mater. Interfaces 2015, 7, 8640−8649

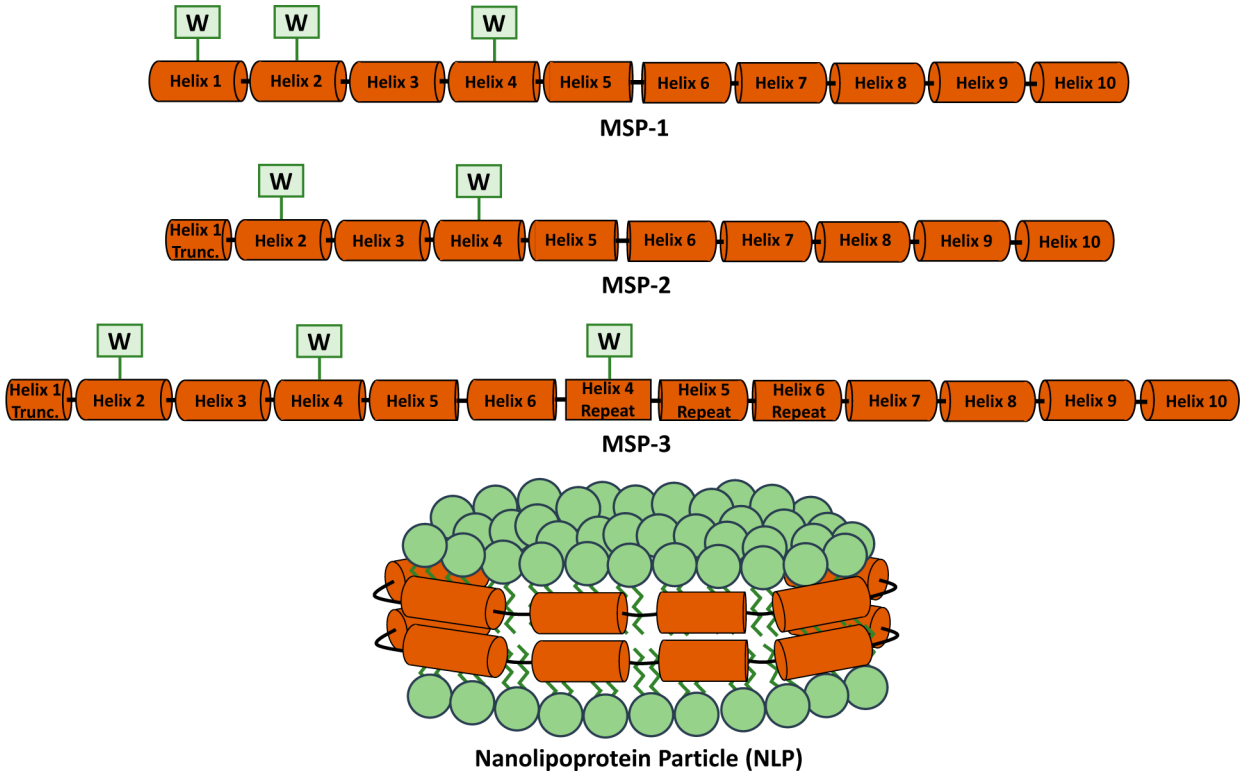

Figure 1. Sequences of the MSPs used and the locations of the tryptophan residues (W) in each one, with the N-terminus located on the left and the C-terminus located on the right. Below is the general structure of an NLP (MSPs bound to lipids).

MD) with a scan range of 190−260 nm at room temperature in a demountable close-ended far-UV 1-mm-path-length quartz cuvette for gel samples and a 1-mm-path-length open-end quartz cuvette for solution samples. CD spectra were normalized by converting the ordinate axis to molar ellipticity.[39] The α-helical content was determined as described elsewhere.[27,39] The concentration of MSP in solution samples was approximately 0.2 mg/mL, while the concentration in silica gel samples was approximately 0.1 mg/mL.

RESULTS AND DISCUSSION

NLPs are self-assembled structures consisting of phospholipids and MSPs and were chosen to be investigated as potential hosts for IMPs because of their size compatibility with mesoporous silica. Although no direct analysis of IMPs was performed in this work, the integrity of MSP−lipid interactions in NLPs was examined. This is important because maintaining the structural integrity of a biological host (i.e., NLPs) would be crucial for its ability to keep IMPs folded correctly in future work. Lipid-free MSPs and MSPs bound to the lipid DMPC were examined in both aqueous solution and mesoporous silica gel for a variety of different analyses. The overall fluorescence emission and quenching of tryptophan residues within the MSPs via acrylamide or nitroxide-spin-labeled stearic acid was investigated, as well as fluorescence anisotropies of these same residues. In addition, the CD spectra of MSPs were recorded and interpreted. All of this analysis was performed to elucidate the structural and conformational changes of MSPs upon entrapment in TMOS-derived, mesoporous silica. Three different MSPs, each derived from the 10 helical regions of Apolipoprotein A-I, were used in this work; MSP-1, MSP-2, and MSP-3 formed NLPs having discoidal diameters of 9.7, 9.2, and 14.8 nm, respectively (see the SI). The structure of each of these MSPs is depicted in Figure 1, where it is shown that each MSP contains tryptophan residues (W) in different positions along the length of the protein belt. These proteins were chosen to provide variability among the positioning and overall solvent accessibility of the tryptophan residues.

Tryptophan fluorescence emission is sensitive to its microenvironment. The maximum emission wavelength is known to undergo a blue shift upon relocation to an environment with decreased polarity[40] (e.g., upon going from an aqueous environment to the tail region of lipid bilayers). The magnitude of this shift for a lipid-free to -bound transition in Apolipoprotein A-I has been observed to be on the order of 2−3 nm.[41] This shift was reproducibly observed for all three of the MSPs utilized in this work, as illustrated in Table 1. MSP-1,

Table 1. Tryptophan Fluorescence Emission Wavelengths (nm) of MSPs in Solution and Silica Gel

	solution		gel	
	lipid-free	lipid-bound	lipid-free	lipid-bound
MSP-1	349	347	346	344
MSP-2	348	345	345	340
MSP-3	346	345	344	340

-2, and -3 exhibited lipid-free to -bound blue shifts of 2, 3, and 1 nm, respectively, in solution while displaying blue shifts of 2, 5, and 4 nm in silica gel. This indicates that the MSPs are interacting with DMPC such that they remain oriented toward the carbon tails, even after entrapment. It is worth noting that, after entrapment, the blue shifts for MSP-2 and -3 (5 and 4 nm, respectively) were of larger magnitude than the blue shift for MSP-1 (2 nm). The larger blue shifts for MSP-2 and -3 were determined to be statistically significant (see the SI). This can perhaps be attributed to the longer Helix 1 and presence of a Helix 1 tryptophan in MSP-1 and absence in MSP-2 and -3

DOI: 10.1021/acsami.5b00898
ACS Appl. Mater. Interfaces 2015, 7, 8640−8649

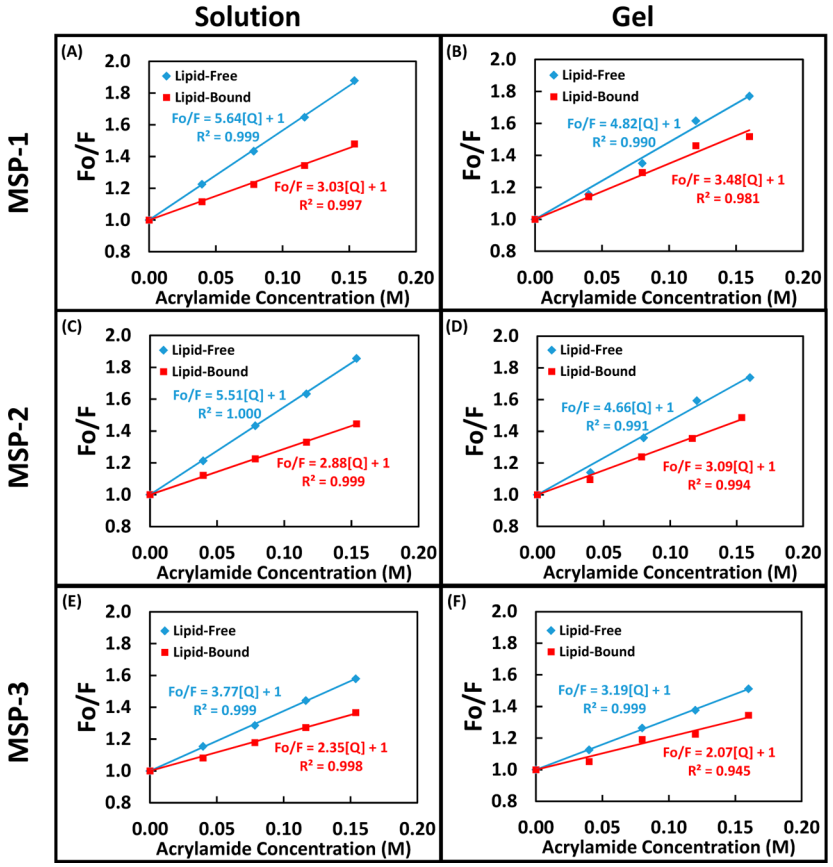

Figure 2. Stern–Volmer plots for lipid-free and -bound (A and B) MSP-1, (C and D) MSP-2, and (E and F) MSP-3, with corresponding regression equations. Measurements are for samples in solution (A, C, and E) and in silica gel (B, D, and F).

(Figure 1). MSP-1 has been shown to exhibit dynamic behavior near its N- and C-termini when bound to lipids (i.e., folded into NLPs) in solution.[42] This dynamic behavior would be associated with the lack of a defined structure in these regions. The blue shift observed for each MSP is the superimposed contribution from each tryptophan residue present in the protein. Therefore, we speculate that for lipid-bound MSP-1 the Helix 1 tryptophan was relatively exposed to the aqueous environment before and after entrapment; this is captured in the statistically similar (see the SI) blue shift for lipid-bound MSP-1. We propose that the relatively shorter Helix 1 of MSP-2 and -3 has less influence upon the lipid-bound MSP structure, allowing the confinement in the gel to impose more structure in lipid-bound MSP-2 and -3, thus resulting in deeper embedding of the Helix 2 and 4 tryptophans (Figure 1) into the bilayer. This is observed as an increased blue shift for MSP-2 and -3. For elucidation of this theory, structural and dynamic characterization of each helix in these lipid-bound MSPs in a gel environment would have to be performed. It can also be seen in Table 1 that the wavelengths of all gel-entrapped MSP emissions were lower in comparison to those in solution. This indicates that the environment within the pores of the silica were less polar than that of solution. This is perhaps due to the residual methanol content [≤5% (v/v)] that remained present after formation of the silica gel monoliths.

Water-soluble acrylamide quenches the fluorescence emission from tryptophan in a proximity-dependent manner.[32] Therefore, the degree of quenching is tied to the local environment of the tryptophan residue, either solvent/water accessible or buried/hydrophobic. The goal of these acrylamide quenching experiments was to compare the quenching behavior of lipid-free and -bound MSPs in solution, observe a difference, and verify that this difference was consistently observed with lipid-free and -bound MSPs in gel. This would strongly suggest that lipid–protein interactions within the NLPs are maintained after gel entrapment. To compare the solvent accessibility of the tryptophan residues for lipid-free and -bound forms of all three MSPs in solution or gel, we created Stern–Volmer plots of tryptophan fluorescence quenching versus acrylamide concentration. The accessibility of acrylamide is encompassed in the Stern–Volmer constant (K_{SV}) obtained through regression of the Stern–Volmer plots using the Stern–Volmer relationship (eq 1). Observing differences among the MSPs was expected because it has been previously shown that tryptophan residues located in different positions along the scaffold protein belt exhibit different quenching behavior.[34,35,43] Figure 2 shows the Stern–Volmer plots with regressed slopes, K_{SV}, for each of the different scaffold proteins in both solution and gel. In all six plots of Figure 2, lipid-free MSPs have larger slopes than the corresponding lipid-bound MSPs under the same conditions, even after gel encapsulation. This strongly suggests that, for each of the three MSPs, the scaffold protein generally remains bound to the lipid after encapsulation. In Table 2, the values of K_{SV} for each MSP are displayed. For MSP-1 and -2, the trends are similar because lipid-free K_{SV} values decreased and lipid-bound K_{SV} values increased (but not significantly) upon entrapment in silica gel. For MSP-3, the K_{SV} values decreased for lipid-free samples but also decreased (but not significantly) for lipid-bound samples once entrapped in the silica gel. The statistical significance of changes in K_{SV} was analyzed (see the

DOI: 10.1021/acsami.5b00898
ACS Appl. Mater. Interfaces 2015, 7, 8640–8649

Table 2. Stern–Volmer Constants (K_{SV}, M^{-1}) of MSPs in Solution and Silica Gel When Quenched by Acrylamide

	solution		gel	
	lipid-free	lipid-bound	lipid-free	lipid-bound
MSP-1	5.64 ± 0.10	3.03 ± 0.11	4.82 ± 0.36	3.48 ± 0.34
MSP-2	5.51 ± 0.08	2.88 ± 0.06	4.66 ± 0.33	3.09 ± 0.15
MSP-3	3.77 ± 0.08	2.35 ± 0.06	3.19 ± 0.08	2.07 ± 0.33

SI), and it was determined that the difference in K_{SV} between a lipid-free and a lipid-bound MSP was significant for all samples. The statistical significance of the differences in the K_{SV} values associated with solution and gel samples was also analyzed; lipid-free MSPs exhibited a significant change in K_{SV}, while lipid-bound MSPs did not. This indicates that the lipid-free MSPs could have undergone significant conformational changes upon entrapment, while the lipid-bound MSPs did not. MSPs are derived from Apolipoprotein A-I, which forms a 4-helix bundle[44] and has relatively dynamic behavior[42] in the lipid-free state in solution. The silica gel entrapment could induce conformational changes in the lipid-free MSPs that alter their structures such that the tryptophan residues become less accessible to water–acrylamide. This speculation is corroborated by previous works where conformational changes in proteins that interact with porous silica surfaces have been observed.[27,45] Table 2 also shows that, for all conditions, the trend $K_{SV,MSP-1} > K_{SV,MSP-2} > K_{SV,MSP-3}$ holds. This is most likely due to the different locations of tryptophan residues in each MSP and the dynamic behavior of the MSPs at the N-terminus;[42] MSP-1 contains two tryptophans near the N-terminus, while MSP-2 and -3 only contain one. Also, MSP-3 contains a tryptophan in the center of the protein belt, far away from each terminus. This would rationalize why, on average, the tryptophans in MSP-1 are the most exposed while the tryptophans in MSP-3 are the least exposed.

Parallax analysis was used to determine the average position of the tryptophan residues of lipid-bound MSPs in solution and in gel with respect to the bilayer center. The helices of MSPs are believed to orient in a manner such that they run perpendicular to the acyl tails of the lipids in the bilayer, as illustrated in Figure 1.[34,35] Therefore, placement of the nitroxide quenchers at different heights in the bilayer results in different quenching efficiencies (i.e., quenchers closer to helices quench tryptophan more so than quenchers farther away). Two forms of lipid partitioning stearic acid were used to achieve this effect. One form had nitroxide covalently attached to the 5-carbon (5-DOXYL), while the other had nitroxide covalently attached to the 16-carbon (16-DOXYL). It is expected that 5-DOXYL and 16-DOXYL would align with their acyl tails parallel to the acyl tails of the lipids in the NLPs. The chemical structures for both of these quenchers are depicted in Figure 3. The ratio of quenching from nitroxides at these different heights can be correlated to the effective height of the tryptophan residues, Z_{eff}, using eq 2. The quenching of tryptophan by 5-DOXYL and 16-DOXYL is shown in Figure 4. For each MSP in both solution and gel, the tryptophan residues were more quenched by 16-DOXYL than 5-DOXYL. This indicates that, on average, the tryptophan residues in each MSP were positioned such that they were closer to the nitroxide spin label on 16-DOXYL (i.e., closer to the bilayer center). Although there is a distinct increase in the fluorescence intensities upon gel entrapment for both 5-DOXYL and 16-DOXYL, there is only a slight increase in the effective height from the bilayer

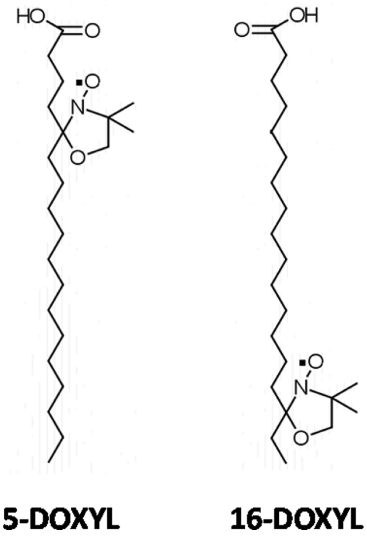

Figure 3. Illustration of the chemical structures of 5-DOXYL and 16-DOXYL.

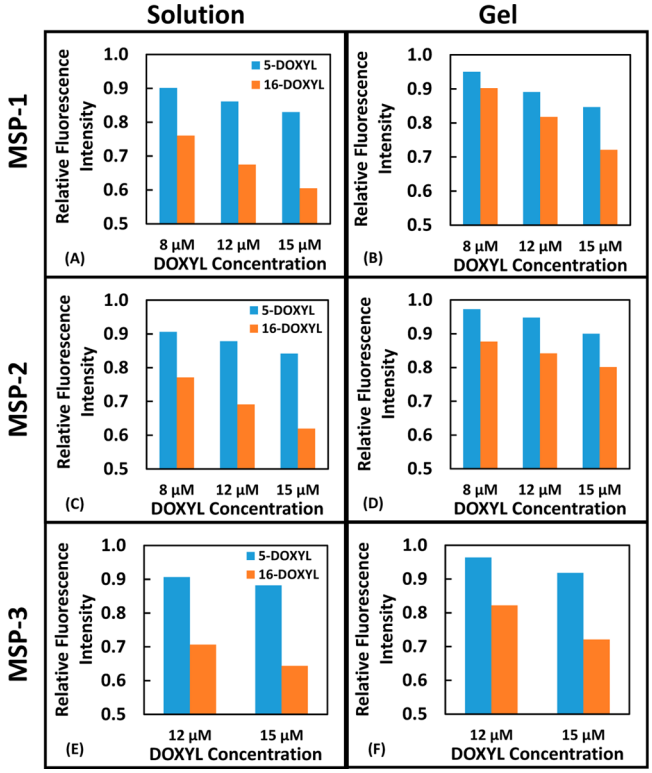

Figure 4. Relative fluorescence intensities of tryptophans in lipid-bound (A and B) MSP-1, (C and D) MSP-2, and (E and F) MSP-3 when quenched by 5-DOXYL and 16-DOXYL at various concentrations. Measurements are for samples in solution (A, C, and E) and in silica gel (B, D, and F).

center (Z_{eff}) for all MSPs, as shown in Table 3. The length of a hydrophobic leaflet on a bilayer is on the order of 15 Å.[46,47] The changes in Z_{eff} upon gel entrapment for MSP-1, -2, and -3 are 0.35, 0.14, and 0.21 Å, respectively. Overall, these displacements are very small in comparison to the size of the leaflet (<3%). All of the values for Z_{eff} in Table 3 are consistent with those in previous works, where it has been shown that Z_{eff} for tryptophan residues can vary from 4.0 to 6.0 Å depending on the tryptophan location in the scaffold protein.[34,35] This

DOI: 10.1021/acsami.5b00898
ACS Appl. Mater. Interfaces 2015, 7, 8640–8649

Table 3. Effective Height (Z_{eff}, Å) of Tryptophan Residues in Lipid-Bound MSPs Determined by Parallax Analysis

	solution	gel
MSP-1	5.73 ± 0.01	6.08 ± 0.05
MSP-2	5.69 ± 0.03	5.83 ± 0.19
MSP-3	4.92 ± 0.05	5.13 ± 0.03

indicates that the MSPs are maintaining a proper lipid-bound conformation after entrapment in silica gel because of the minimal change in the positioning of the tryptophan residues.

The fluorescence anisotropy of tryptophan in lipid-free and -bound MSPs in both solution and silica gel was analyzed by eq 3. Fluorescence anisotropy is a measure of the rotational freedom of a molecule, which is directly related to its size or the size of the aggregate it is associated with.[38] In Figure 5, it is

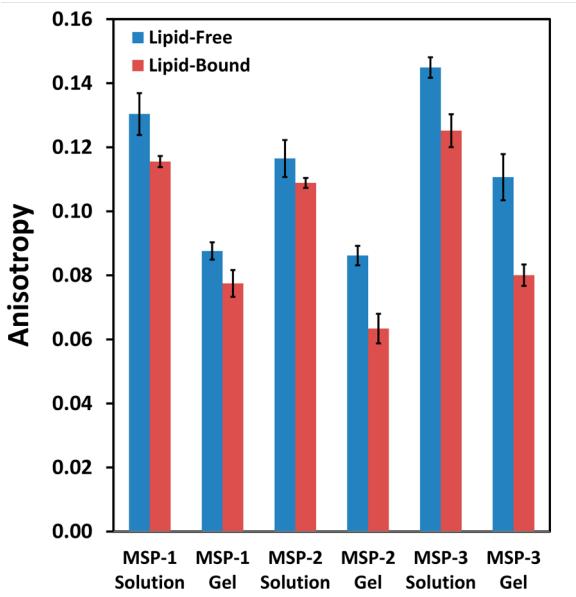

Figure 5. Fluorescence anisotropy values of lipid-free and -bound MSPs in solution and silica gel.

shown that the anisotropy of each lipid-free MSP is higher than that of its corresponding lipid-bound MSP in both solution and gel. This difference in the anisotropy was determined to be statistically significant (see the SI). This indicates that the lipid-free assemblies are larger than the lipid-bound assemblies because of their slower rotational speed. This is counterintuitive because one would expect a single protein to be smaller than a protein−lipid assembly consisting of two proteins and a few hundred lipids. However, in solution, MSPs exist as oligomers;[30,41] these oligomers are capable of being larger than NLPs. Using dynamic light scattering, we have confirmed that this is the case because lipid-free MSPs display a heterogeneous size distribution with many populations larger than the homogeneously dispersed lipid-bound population (see the SI). There is a decrease in the anisotropy for all MSP samples once entrapped in silica gel, as shown in Figure 5. This change in the anisotropy was also determined to be statistically significant (see the SI). Again, this decrease in the anisotropy is counterintuitive because of the apparent increased motion in a confined environment. We speculate that this is the result of large lipid-free MSP oligomers breaking down into smaller ones and NLPs remodeling upon entrapment into smaller particles. The magnitude of the size decrease cannot be determined from our experimental methods. However, our previous work, in which the lipid phase behavior of silica-gel entrapped NLPs belted by MSP-3 was investigated, corroborates the theory of NLP shrinkage upon entrapment.[27]

CD spectroscopy was used to examine the secondary structures of MSP-1 and -2 and how they changed upon entrapment. Figure 6 shows the spectra of lipid-free and -bound MSP-1 and -2 in solution and in silica gel. Spectra were not recorded for MSP-3 because we had previously investigated and reported this.[27] All spectra show a curve with two minima at 208 and 222 nm, which is indicative of strong α-helical content.[48] The corresponding α-helical content is shown in Table 4. Parts A and C of Figure 6 show that MSP-1 and -2, respectively, underwent an increase in the molar ellipticity when bound to lipids. This corresponds to an increase in the α-helical content, which is shown in Table 4 to be 50−72% for MSP-1 and 48−70% for MSP-2. This increase in the α-helical content is consistent with previous works in which Apolipoprotein A-I and other MSPs were examined.[27,30,42,49,50]

A similar lipid-induced shift in the molar ellipticity of the scaffold protein occurred for NLPs entrapped in the silica gel (Figure 6B,D). Thus, the results from CD analyses also indicate that the MSP maintains its interactions with the lipids when embedded in the mesoporous sol−gel matrix.

Interestingly, silica gel entrapment increased the α-helical content of lipid-free MSP-1 and -2 (50−60% for MSP-1 and 48−58% for MSP-2). However, the lipid-bound forms remain almost the same (72−70% for MSP-1 and 70−72% for MSP-2). This shows that the lipid-free MSPs adopt a more helical structure in the gel, while the lipid-bound MSPs remain relatively unchanged. This is consistent with our previous CD spectroscopy work using MSP-3, where gel entrapment seemed to increase the α-helical content of lipid-free MSP-3 but not that for the lipid-bound form significantly.[27] This is also corroborated by the acrylamide quenching experiments performed in this work, where the significant decrease in K_{SV} for lipid-free MSPs suggests a more compact structure in the silica gel. On the other hand, the lack of a significant change in K_{SV} for lipid-bound MSPs is consistent with maintenance of the α-helical content following gel entrapment. Although the speculated size change of NLPs appears to have no effect on the lipid-bound MSP structure, perhaps the breaking down of larger lipid-free MSP aggregates into smaller ones permits the formation of structures with higher α-helical content, as suggested by the fluorescence anisotropy and CD measurements. Molecular crowding (volume exclusion) effects of gel entrapment may also drive an increase in the α-helical content of the lipid-free protein.[51] It is worth noting that, in Figure 6, both MSP-1 and MSP-2 seem to exhibit inversion in their peak heights at 208 and 222 nm after silica gel entrapment. Table 5 shows the 222/208 ratio for each sample before and after entrapment. All solution samples have a 222/208 ratio under 1, which is indicative of isolated helixes.[52] All of the gel samples have a 222/208 ratio above 1. Although 222/208 ratios above 1 typically indicate the presence of a coiled-coil structure,[52] a coiled-coil motif would not be justified in the context of our results. For example, a coiled-coil would require the scaffold proteins on an NLP to come into very close proximity of one another. However, parallax analysis shows that they actually go slightly farther away from one another. Interparticle protein interactions could result in coiled-coils. However, this would indicate that the particles aggregate, thus, on average, becoming

DOI: 10.1021/acsami.5b00898
ACS Appl. Mater. Interfaces 2015, 7, 8640−8649

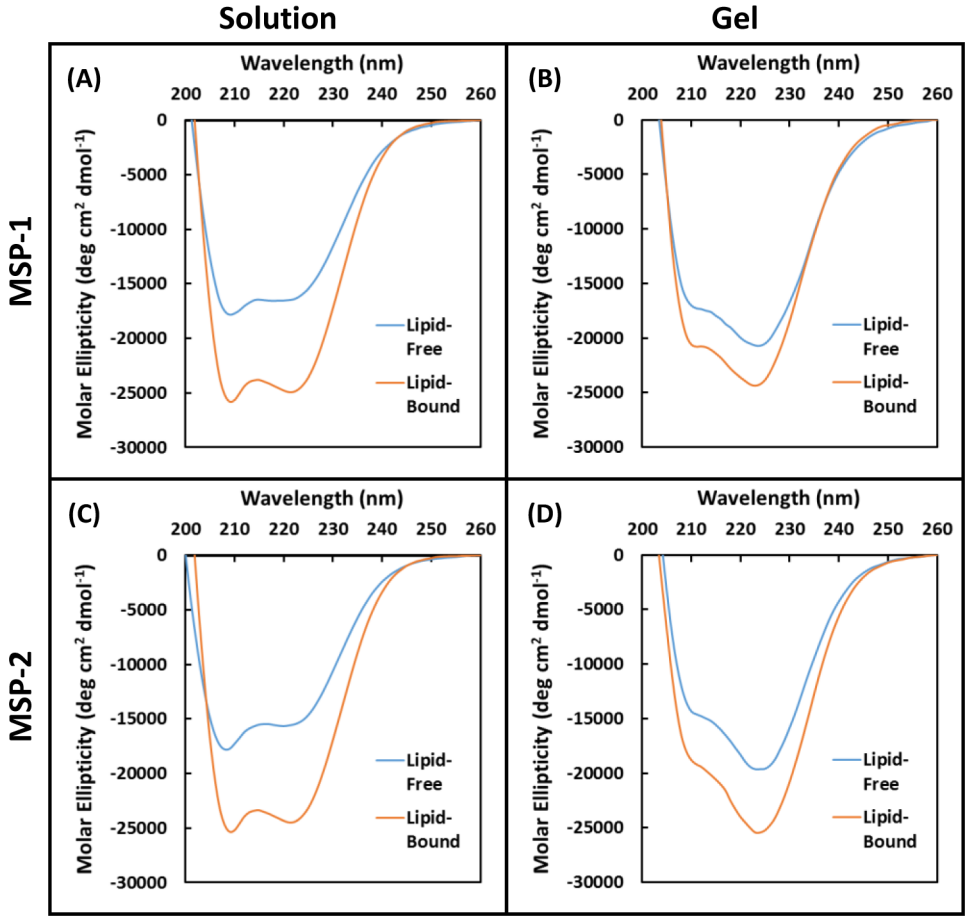

Figure 6. CD spectra of lipid-free and -bound (A) MSP-1 in solution, (B) MSP-1 in silica gel, (C) MSP-2 in solution, and (D) MSP-2 in silica gel.

Table 4. α-Helical Content (%) of MSPs Determined from 222 nm Molar Ellipticity in CD Spectra

	lipid-free	lipid-bound
MSP-1 solution	50	72
MSP-1 gel	60	70
MSP-2 solution	48	70
MSP-2 gel	58	72

Table 5. 222/208 Peak Ratio from CD Spectra for MSPs in Solution and Gel

	lipid-free	lipid-bound
MSP-1 solution	0.94	0.99
MSP-1 gel	1.35	1.34
MSP-2 solution	0.87	0.99
MSP-2 gel	1.61	1.51

larger. The fluorescence anisotropy of entrapped NLPs showed that this is not the case because they may potentially decrease in size after entrapment. We speculate that this inversion in the 222/208 ratio could be a result of interactions of MSP-1 and -2 with the silica gel. The extent and type of interactions involved cannot be determined from this current work and would require further investigation. In our previous work, MSP-3 was utilized as a scaffold protein and also seemed to exhibit a 222/208 ratio inversion after gel entrapment.[27] However, this inversion was of a smaller magnitude. In solution, 222/208 ratios were 0.87 and 0.91 for lipid-free and -bound samples, respectively. After entrapment in silica gel, both samples exhibited a 222/208 ratio of approximately 1. On the basis of our analysis, it is difficult to resolve the reasoning for the difference in the CD spectral behavior between MSP-1/2 and MSP-3. It could perhaps be related to the size difference between MSP-1/2 and MSP-3. This 222/208 ratio inversion behavior, however, should not detract from the main message of our CD spectroscopy findings; MSP-1 and -2 both exhibit increased α-helical content when going from a lipid-free to a lipid-bound conformation in solution, and this behavior is consistently observed in gelled samples.

In previous work, we demonstrated that NLPs made using MSP-3 exhibited stability after silica gel entrapment for at least 5−6 weeks.[27] The long-term stability of the NLPs examined in this work was not studied. However, on the basis of the general similarities in behavior observed between the three MSPs in this work, we speculate that NLPs synthesized with MSP-1 and -2 are capable of exhibiting time scales of stability similar to those observed with MSP-3. Further analysis would need to be performed in order to assess this prediction.

CONCLUSIONS

We have shown that, for three different MSPs associated with NLPs, the protein−lipid interactions were retained upon entrapment in TMOS-derived silica gel. The MSPs examined maintained an orientation in which they were buried in hydrophobic lipid tails. This was determined by using fluorescence spectroscopy and quenching of tryptophan with acrylamide. Fluorescence spectroscopy showed consistent blue shifts in tryptophan emission when lipid-free MSP spectra are

DOI: 10.1021/acsami.5b00898
ACS Appl. Mater. Interfaces 2015, 7, 8640−8649

compared to lipid-bound MSP spectra, which is consistent with MSPs being in a more hydrophobic environment. Fluorescence quenching of the tryptophan residues with acrylamide showed that lipid-bound MSPs had an orientation in which they were less exposed to solvent than lipid-free MSPs. Thus, again, they were most likely buried in the lipid tails. Fluorescence quenching using 5-DOXYL-stearic acid and 16-DOXYL-stearic acid showed that lipid-bound MSPs were positioned at a distance of 5−6 Å away from the bilayer center in solution and maintained that distance of separation after entrapment. Fluorescence anisotropy revealed that NLPs were smaller in size than lipid-free MSP oligomers in both solution and gel and that both experienced some degree of shrinkage upon entrapment possible because of structural reorganization. CD spectroscopy demonstrated that lipid-bound MSPs possessed a higher degree of α-helical content in solution than lipid-free MSPs (∼70% for lipid-bound and ∼50% for lipid-free) and that this higher degree was retained after entrapment (∼70% for lipid-bound and ∼60% for lipid-free). A higher percentage of α-helical content is associated with protein−lipid interactions in NLPs. The combination of various fluorescence spectroscopic techniques and CD spectroscopy illustrated that, after entrapment, lipid-bound MSPs exhibited much fewer significant structural and dynamic changes than lipid-free MSPs because of stabilization from the protein−lipid interactions. Our spectroscopic analyses confirmed that MSPs indeed continued to interact with lipids in NLPs after entrapment with minimal change. In combination with our previous work, we have demonstrated that NLPs are viable biological membrane hosts for silica gel entrapment and more suitable than liposomes. This sets precedent for future work utilizing IMPs incorporated into NLPs to synthesize functional biomaterials derived from sol−gel encapsulation.

■ ASSOCIATED CONTENT

Supporting Information

Additional details of fluorescence emission spectral analysis methods and statistical analysis, including all regressed spectral data from the quenching of tryptophan fluorescence by acrylamide, N_2 adsorption isotherm data used to determine the silica gel pore size, and graphical dynamic light scattering data used to characterize MSP aggregates and NLP diameters. This material is available free of charge via the Internet at http://pubs.acs.org.

■ AUTHOR INFORMATION

Corresponding Author

*E-mail: mllongo@ucdavis.edu.

Notes

The authors declare no competing financial interest.

■ ACKNOWLEDGMENTS

We are grateful to Atul Parikh, Steven Theg, and Ricardo Castro for use of experimental facilities. W.F.Z. and S.H. were supported by Grant T32-GM008799 from NIGMS−NIH. The content of this Article is solely the responsibility of the authors and does not necessarily represent the official views of the NIGMS or NIH.

■ REFERENCES

(1) Ruiz-Hitzky, E.; Ariga, K.; Lvov, Y. *Bio-Inorganic Hybrid Nanomaterials: Strategies, Syntheses, Characterization and Applications*; Wiley-VCH: Weinheim, Germany, 2008.
(2) Avnir, D.; Coradin, T.; Lev, O.; Livage, J. Recent Bio-Applications of Sol−Gel Materials. *J. Mater. Chem.* **2006**, *16*, 1013.
(3) Schlipf, D. M.; Rankin, S. E.; Knutson, B. L. Pore-Size Dependent Protein Adsorption and Protection from Proteolytic Hydrolysis in Tailored Mesoporous Silica Particles. *ACS Appl. Mater. Interfaces* **2013**, *5*, 10111−10117.
(4) Nassif, N.; Livage, J. From Diatoms to Silica-Based Biohybrids. *Chem. Soc. Rev.* **2011**, *40*, 849−59.
(5) Kato, M.; Sakai-Kato, K.; Toyo'oka, T. Silica Sol−Gel Monolithic Materials and Their Use in a Variety of Applications. *J. Sep. Sci.* **2005**, *28*, 1893−1908.
(6) Monton, M. R. N.; Forsberg, E. M.; Brennan, J. D. Tailoring Sol−Gel Derived Silica Materials for Optical Biosensing. *Chem. Mater.* **2012**, *24*, 796−811.
(7) Brennan, J. D. Biofriendly Sol−Gel Processing for Entrapment of Soluble and Membrane-Bound Proteins: Toward Novel Solid-Phase Assays for High-Throughput Screening. *Acc. Chem. Res.* **2007**, *40*, 827−835.
(8) Brown, B. S. *Biological Membranes*; Biochemical Society: London, 1996.
(9) Goodman, S. R. *Medical Cell Biology*; Academic Press: Waltham, MA, 2007.
(10) Mitchell, D. C.; Lawrence, J. T. R.; Litman, B. J. Primary Alcohols Modulate the Activation of the G Protein-Coupled Receptor Rhodopsin by a Lipid-Mediated Mechanism. *J. Biol. Chem.* **1996**, *271*, 19033−19036.
(11) Lucero, P.; Penalver, E.; Monero, E.; Lagunas, R. Moderate Concentrations of Ethanol Inhibit Endocytosis of the Yeast Maltose Transporter. *Appl. Environ. Microbiol.* **1997**, *63*, 3831−3836.
(12) Lu, J. Z.; Huang, F.; Chen, J. W. The Behaviors of the Ca^{2+} Atpase Embedded in Interdigitated Bilayer. *J. Biochem.* **1999**, *126*, 302−306.
(13) Avdulov, N. A.; Chochina, S. V.; Draski, L. J.; Deitrich, R. A.; Wood, W. G. Chronic Ethanol Consumption Alters Effects of Ethanol in Vitro on Brain Membrane Structure of High Alcohol Sensitivity and Low Alcohol Sensitivity Rats. *Alcohol.: Clin. Exp. Res.* **1995**, *19*, 886−891.
(14) Shen, C.; Kostic, N. M. Kinetics of Photoinduced Electron Transfer Reactions within Sol−Gel Silica Glass Doped with Zinc Cytochrome C. *J. Am. Chem. Soc.* **1997**, *119*, 1304−1312.
(15) Gottfried, D. S.; Kagan, A.; Hoffman, B. M.; Freidman, J. M. Impeded Rotation of a Protein in a Sol−Gel Matrix. *J. Phys. Chem. B* **1999**, *103*, 2803−2807.
(16) Baker, G. A.; Jordan, J. D.; Bright, F. V. Effects of Poly(Ethylene Glycol) Doping on the Behavior of Pyrene, Rhodamine 6g, and Acrylodan-Labeled Bovine Serum Albumin Sequestered within Teteramethylorthosilane-Derived Sol−Gel-Processed Composites. *J. Sol−Gel Sci. Tecnol.* **1998**, *11*, 43−54.
(17) Flora, K. K.; Brennan, J. D. Effect of Matrix Aging on the Behaviour of Human Serum Albumin Entrapped in a Tetraethylorthosilicate-Derived Glass. *Chem. Mater.* **2001**, *13*, 4170−4179.
(18) Eggers, D. K.; Valentine, J. S. Crowding and Hydration Effects on Protein Conformation: A Study with Sol−Gel Encapsulated Proteins. *J. Mol. Biol.* **2001**, *314*, 911−922.
(19) Brennan, J. D.; Benjamin, D.; Dibattista, E.; Gulcev, M. D. Using Sugar and Amino Acid Additives to Stabilize Enzymes within Sol−Gel Derived Silica. *Chem. Mater.* **2003**, *15*, 737−745.
(20) Brinker, C. J.; Scherer, G. W. *Sol−Gel Science: The Physics and Chemistry of Sol−Gel Processing*; Academic Press: San Diego, CA, 1990; pp 108−216.
(21) Slater, J. L.; Huang, C. Interdigitated Bilayer Membranes. *Prog. Lipid Res.* **1988**, *27*, 325−359.
(22) Tierney, K. J.; Block, D. E.; Longo, M. L. Elasticity and Phase Behavior of DPPC Membrane Modulated by Cholesterol, Ergosterol, and Ethanol. *Biophys. J.* **2005**, *89*, 2481−2493.

DOI: 10.1021/acsami.5b00898
ACS Appl. Mater. Interfaces 2015, 7, 8640−8649

(23) Brook, M. A.; Chen, Y.; Guo, K.; Zhang, Z.; Brennan, J. D. Sugar-Modified Silanes: Precursors for Silica Monoliths. *J. Mater. Chem.* **2004**, *14*, 1469−1479.
(24) Chen, Y.; Zhang, Z.; Sui, X. H.; Brennan, J. D. Reduced Shrinkage of Sol−Gel Derived Silicas Using Sugar-Based Silsequioxane Precursors. *J. Mater. Chem.* **2005**, *15*, 3132−3141.
(25) Besanger, T.; Zhang, Y.; Brennan, J. D. Characterization of Fluorescent Phospholipid Liposomes Entrapped in Sol−Gel Derived Silica. *J. Phys. Chem. B* **2002**, *106*, 10535−10542.
(26) Bricarello, D. A.; Smilowitz, J. T.; Zivkovic, A. M.; German, J. B.; Parikh, A. N. Reconstituted Lipoprotein: A Versatile Class of Biologically-Inspired Nanostructures. *ACS Nano* **2011**, *5*, 42−57.
(27) Zeno, W. F.; Hilt, S. L.; Aravagiri, K. A.; Risbud, S. H.; Voss, J. C.; Parikh, A. N.; Longo, M. L. Analysis of Lipid Phase Behavior and Protein Conformational Changes in Nanolipoprotein Particles Upon Entrapment in Sol−Gel-Derived Silica. *Langmuir* **2014**, *30*, 9780−9788.
(28) Ferrer, M.; Del Monte, F.; Levy, D. A. A Novel and Simple Alcohol Free Sol Gel Route for Encapsulation of Labile Proteins. *Chem. Mater.* **2002**, *14*, 3619−3621.
(29) Luo, T. J.; Soong, R.; Lan, E.; Dunn, B.; Montemagno, C. Photo-Induced Proton Gradients and ATP Biosynthesis Produced by Vesicles Encapsulated in a Silica Matrix. *Nat. Mater.* **2005**, *4*, 220−224.
(30) Bayburt, T. H.; Grinkova, Y. V.; Sligar, S. G. Self-Assembly of Discoidal Phospholipid Bilayer Nanoparticles with Membrane Scaffold Proteins. *ACS Nano* **2002**, *2*, 853−856.
(31) Denisov, I. G.; Grinkova, Y. V.; Lazarides, A. A.; Sligar, S. G. Directed Self-Assembly of Monodisperse Phospholipid Bilayer Nanodiscs with Controlled Size. *J. Am. Chem. Soc.* **2004**, *126*, 3477−3487.
(32) Lehrer, S. S. Solute Perturbaiton of Protein Fluorescence. The Quenching of the Tryptophyl Fluorescence of Model Compounds and of Lysozyme by Iodide Ion. *Biochemistry* **1971**, *10*, 3254−3263.
(33) Oda, M. N.; Budamagunta, M. S.; Geier, E. G.; Chandradas, S. H.; Shao, B.; Heinecke, J. W.; Voss, J. C.; Cavigiolio, G. Conservation of Apolipoprotein A-I's Central Domain Structural Elements upon Lipid Association on Different High-Density Lipoprotein Subclasses. *Biochemistry* **2013**, *52*, 6766−6778.
(34) Panagotopulos, S. E.; Horace, E. M.; Moiorano, J. N.; Davidson, W. S. Apolipoprotein AI Adopts a Belt-Like Orientation in Reconstituted High Density Lipoproteins. *J. Biol. Chem.* **2001**, *276*, 42965−42970.
(35) Moiorano, J. N.; Davidson, W. S. The Orientation of Helix 4 in Apolipoprotein AI-Containing Reconstituted High Density Lipoproteins. *J. Biol. Chem.* **2000**, *275*, 17374−17380.
(36) Ladokhin, A. S. Analysis of Protein and Peptide Penetration into Membranes by Depth-Dependent Fluorescence Quenching: Theoretical Considerations. *Biophys. J.* **1999**, *76*, 946−955.
(37) Ren, J.; Lew, S.; Wang, Z.; London, E. Transmembrane Orientation of Hydrophobic Alpha-Helices Is Regulated Both by the Relationship of Helix Length to Bilayer Thickness and by the Cholesterol Concentration. *Biochemistry* **1997**, *36*, 10213−10220.
(38) Lakowicz, J. *Principles of Fluorescence Spectroscopy*; Springer: New York, 2006.
(39) Morrow, J. A.; Segall, M. L.; Lund-Katz, S.; Phillips, M. C.; Knapp, M.; B, R.; Weisgraber, K. H. Differences in Stability among the Huan Apolipoprotein E Isoforms Determined by the Amino-Terminal Domain. *Biochemistry* **2000**, *39*, 11657−11666.
(40) Caputo, G. A.; London, E. Cumulative Effects of Amino Acid Substitutions and Hydrophobic Mismatch Upon the Transmembrane Stability and Conformation of Hydrophobic Alpha-Helices. *Biochemistry* **2003**, *42*, 3275−3285.
(41) Davidson, W. S.; Hazlett, T.; Mantulin, W. W.; Jonas, A. The Role of Apolipoprotein AI Domains in Lipid Binding. *Proc. Natl. Acad. Sci. U.S.A.* **1996**, *93*, 13605−13610.
(42) Morgan, C. R.; Hebling, C. M.; Rand, K. D.; Stafford, D. W.; Jorgenson, J. W.; Engen, J. R. Conformational Transitions in the Membrane Scaffold Protein of Phospholipid Bilayer Nanodiscs. *Mol. Cell. Proteomics* **2011**, *10*, M111−010876.
(43) Caputo, G. A.; London, E. Using a Novel Dual Fluorescence Quenching Assay for Measurement of Tryptophan Depth within Lipid Bilayers to Determine Hydrophobic Alpha-Helix Locations within Membranes. *Biochemistry* **2003**, *42*, 3265−3274.
(44) Pollard, R. D.; Fulp, B.; Samuel, M. P.; Sorci-Thomas, M. G.; Thomas, M. J. The Conformation of Lipid-Free Human Apolipoprotein A-I in Solution. *Biochemistry* **2013**, *52*, 9470−81.
(45) Eggers, D. K.; Valentine, J. S. Molecular Confinement Influences Protein Structure and Enhances Thermal Protein Stability. *Protein Sci.* **2001**, *10*, 250−261.
(46) Rawicz, W.; Olbrich, K. C.; McIntosh, T.; Needham, D.; Evans, E. Effect of Chain Length and Unsaturation on Elasticity of Lipid Bilayers. *Biophys. J.* **2000**, *79*, 328−339.
(47) Lewis, B. A.; Engelman, D. M. Lipid Bilayer Thickness Varies Linearly with Acyl Chain Length in Fluid Phosphatidylcholine Vesicles. *J. Mol. Biol.* **1983**, *166*, 211−217.
(48) Kelly, S. M.; Jess, T. J. How to Study Proteins by Circular Dichroism. *Biochim. Biophys. Acta* **2005**, *1751*, 119−139.
(49) Alexander, E. T.; Tanaka, M.; Kono, M.; Saito, H.; Rader, D. J.; Phillips, M. C. Structural and Functional Consequences of the Milano Mutation (R173c) in Human Apolipoprotein AI. *J. Lipid Res.* **2009**, *50*, 1409−1419.
(50) Petrlova, J.; Dalla-Riva, J.; Mörgelin, M.; Lindahl, M.; Krupinska, E.; Stenkula, K. G.; Voss, J. C.; Lagerstedt, J. O. Secondary Structure Changes in Apoa-I Milano (R173c) Are Not Accompanied by a Decrease in Protein Stability or Solubility. *PLoS One* **2014**, *9*, e96150.
(51) Zhou, H. X. Influence of Crowded Cellular Environments on Protein Folding, Binding, and Oligomerization: Biological Consequences and Potentials of Atomistic Modeling. *FEBS lett.* **2013**, *587*, 1053−1061.
(52) Zhou, N. E.; Kay, C. M.; Hodges, R. S. Synthetic Model Proteins. Positional Effects of Interchain Hydrophobic Interactions on Stability of Two-Stranded Alpha-Helical Coiled-Coils. *J. Biol. Chem.* **1992**, *267*, 2664−2670.

DOI: 10.1021/acsami.5b00898
ACS Appl. Mater. Interfaces 2015, 7, 8640−8649